ORIGINAL RESEARCH

Pattern Electroretinogram Parameters and their Associations with Optical Coherence Tomography in Glaucoma Suspects

Andrew Tirsi[1], Amanda Wong[2], Daniel Zhu[3], Guillaume Stoffels[4], Peter Derr[5], Celso Tello MD[6]

Received on: 31 August 2021; *Accepted on:* 06 December 2021; *Published on:* 30 August 2022

Abstract

Aim: To investigate whether steady state pattern electroretinogram (ssPERG) could identify retinal ganglion cell (RGC) dysfunction, and to assess the relationship between ssPERG with optical coherence tomography (OCT) measurements in glaucoma suspects (GS).

Materials and methods: This was a prospective cohort study of GS, identified based on suspicious optic disk appearance and glaucoma risk factors. Complete eye exam, Standard automated perimetry, OCT, and ssPERG were performed. Magnitude (Mag), Magnitude D (MagD), and MagD/Mag ratio were subsequently used in the correlation and linear regression analyses between ssPERG parameters and the RNFL, GCL/IPL, and macular thicknesses measurements.

Results: Forty-nine eyes of 26 patients were included. Mag and MagD were significantly correlated with the superior, inferior, and average RNFL thicknesses (avRNFLT). All ssPERG parameters were significantly correlated with the average and minimum GCL/IPL thicknesses and the inner macular sector thicknesses. Mag and MagD significantly predicted the superior, inferior, and avRNFLT in the regression analysis. All ssPERG parameters were predictive of GCL/IPL thickness in all sectors as well as the average and minimum GCL/IPL thicknesses. All ssPERG parameters were predictive of all inner macular sector thicknesses and MagD was also predictive of some outer macular sector thicknesses as well.

Conclusion: ssPERG has significant correlations with and is predictive of RNFL, GCL/IPL, and macular thicknesses in glaucoma suspects.

Clinical significance: ssPERG may serve as a useful objective functional tool for identifying and following the progression of disease in glaucoma suspects.

Keywords: Ganglion cell layer, Glaucoma, Glaucoma suspect, Inner plexiform layer, Macula, Optic nerve, Optical coherence tomography, Retinal ganglion cell, Retinal nerve fiber layer, Steady state pattern electroretinogram.

Journal of Current Glaucoma Practice (2022): 10.5005/jp-journals-10078-1365

Introduction

Glaucoma is characterized by progressive visual loss secondary to irreversible retinal ganglion cell (RGC) dysfunction and death secondary to cellular and environmental stressors.[1] The inner layers of the retina, the ganglion cell, and inner plexiform layers (GCL/IPL), have been proposed to be the preferred location for damage in glaucomatous eyes.[2] It has also been demonstrated that there is a significant positive correlation between GCL/IPL thickness and the amplitude of pattern electroretinogram (PERG) of early glaucoma patients and this correlation was apparent prior to any detectable changes in the visual fields (VF) of patients.[3,4] These findings suggest that PERG may serve as a more sensitive screening test for patients with early glaucoma compared to current methods, which have limited efficacy and variable accuracy in this population.[5]

Previous studies have also reported on the associations between PERG and the thicknesses of the retinal nerve fiber layer (RNFL) and macular thicknesses in glaucoma patients.[3,4,6] PERG has also been found to predict rim area loss in preperimetric glaucoma patients after controlling for disk area.[7] However, to our knowledge no studies have investigated the utility of PERG parameters for predicting structural changes on SD-OCT of all the macular, RNFL, and GCL/IPL sector thicknesses in glaucoma suspects. Whereas VF can be utilized as a functional test that can be correlated with structural damage for glaucoma patients, many glaucoma suspects patients have normal VFs,[8,9] and at least 25% of RGC must be lost to detect a significant change on perimetry.[10] Therefore, PERG may serve as a promising tool to bridge the gap and allow for the detection of visual dysfunction in glaucoma suspects. In recent years, steady state PERG (ssPERG) with the facilitated acquisition, interpretation, and improved subject comfort, was introduced.[11] Additional filters and amplifiers were used to achieve adequate levels of amplitude and

[1,6]Department of Ophthalmology, Manhattan Eye, Ear, & Throat Hospital, Northwell Health, New York, United States; Donald and Barbara Zucker School of Medicine at Hofstra/Northwell, Hempstead, New York, United States

[2,3]Donald and Barbara Zucker School of Medicine at Hofstra/Northwell, Hempstead, New York, United States

[4]Lennox Hill Hospital/Northwell, Feinstein Institute for Medical Research, New York, United States

[5]Diopsys, Inc., Pine Brook, NJ, United States

Corresponding Author: Andrew Tirsi, Department of Ophthalmology, Manhattan Eye, Ear, & Throat Hospital, Northwell Health, New York, United States; Donald and Barbara Zucker School of Medicine at Hofstra/Northwell, Hempstead, New York, United States, Phone: 1 (201) 982 4168, e-mail: atirsi@northwell.edu

How to cite this article: Tirsi A, Wong A, Zhu D, *et al.* Pattern Electroretinogram Parameters and their Associations with Optical Coherence Tomography in Glaucoma Suspects. J Curr Glaucoma Pract 2022;16(2):96–104.

Source of support: Nil

Conflict of interest: Dr. Andrew Tirsi and Dr. Celso Tello are consultants for Diopsys, Inc. Peter Derr is an employee at Diopsys, Inc.

signal-to-noise ratio (SNR) to allow interpretation of the readings. These studies suggested that the PERGLA protocol introduced by Porciatti et al. earlier[12] could be used as a potential alternative to the classic PERG protocol in a clinical setting,[11,13,14] and data interpretation using Fourier analysis in the PERGLA ssPERG is identical to the ISCEV recommendations.[11,15,16] In recent years, the new office-based device, the Diopsys NOVA (Diopsys Inc., NJ) using the PERGLA protocol was introduced, with new validated proprietary parameters [Magnitude (Mag), MagnitudeD (MagD) and MagD/Mag ratio] to assess RGC function.[11] They concluded that ssPERG parameters were repeatable, reproducible, and reliable to be used in clinical settings.[11,17,18] In another study, Porciatti et al. demonstrated that ssPERG amplitude and phase were essentially uncoupled, implying that these measures reflected distinct different aspects of RGC functional activity.[12]

The purpose of this present study was to investigate the relationship between ssPERG parameters and the SD-OCT thickness measurements of inner retinal layers in glaucoma suspects and to determine their individual contributions to the effects of RGC dysfunction on structural measures.

Materials and Methods

In this prospective cross-sectional study, a total of 26 eligible glaucoma suspects (49 eyes) were recruited from the Manhattan Eye, Ear & Throat Hospital ophthalmology practice and underwent a complete ophthalmologic examination, including slit-lamp biomicroscopy, Goldmann tonometry, standard automated perimetry (Humphrey Field Analyzer II, 24-2 and 10-2 SITA-Standard strategy), OCT (Carl Zeiss Meditec Inc., Dublin, CA, USA) and steady state PERG (ssPERG) (Diopsys Inc., Pine Brook, NJ, USA). The study was approved by the Institutional Review Board of Northwell Health System. Written informed consent was obtained from all subjects and the study adhered to the tenets of the Declaration of Helsinki.

Study participants satisfied the following criteria: participants were 40–80 years old and had a best-corrected visual acuity better or equal to 20/40 as measured by Snellen visual acuity testing at the time of enrollment. All participants had a suspicious glaucomatous optic nerve head appearance (increased cup to disk ratio >0.4, or neuroretinal rim thinning, notching, or excavation), and a documented and repeatable normal Humphrey Field Analyzer (HFA) 24-2 at the baseline visit. All participants were not on intraocular pressure-lowering treatment at the time of enrollment. All individuals with prior intraocular or posterior segment intraocular surgery, ocular trauma, or ocular or systemic conditions that may affect optic nerve head structure and/or function, except for uncomplicated cataract extraction with posterior chamber intraocular lens implant and no escape of vitreous to the anterior chamber performed less than a year before enrollment, were excluded from this study.

Spectral-domain Optical Coherence Tomography

Average and in quadrant retinal nerve fiber layer thicknesses (avRNFLT), average, sectorial, and minimum GCIPLT were measured using the Optic Disk Cube protocol of a Cirrus spectral-domain optical coherence tomography (SD-OCT) version 6.0. as described elsewhere.[19]

Visual Field Testing

All patients underwent standard automated perimetry (SAP) testing using the HFA 24-2 and 10–2 protocols. Visual fields with more than 20% fixation losses, false-negative errors, and false-positive errors were excluded. Only participants with visual fields corresponding to stage 0 (no visual field losses) following the Glaucoma Staging System 2 (GSS 2) were considered.[19]

ssPERG Testing

The steady state PERG (ssPERG) was recorded using a commercially available system, Diopsys® NOVA-PERG (Diopsys, Inc. Pine Brook, New Jersey, USA). ssPERG measurements from Diopsys® are based on normative data from healthy subjects.[20] Tests were performed in a dark room to standardized environment luminance, free of visual, and audible distractions. The patient's seat height was adjusted so the tested eye stayed in a horizontal plane with the center of the monitor. The forehead skin was cleaned using NuPerp® Skin Prep Gel (Weaver and Company, CO, USA) and the lower eyelids using OCuSOFT® Lid Scrub Original (OCuSOFT® Inc., Rosenberg, TX, USA) to ensure good and stable electrical activity. Disposable hypoallergenic skin sensors Silver/Silver Chloride ink (Diopsys® proprietary Skin Sensor) were applied on the lower lid of both eyes, close to the lid margin and avoiding eyelashes. One ground sensor (Diopsys® EEG electrode) was applied in the central forehead area with a small amount of conductive paste (Ten20®, Weaver, and Company) and cables from the Diopsys NOVA device were connected to the electrodes. A total of three electrodes were used per test per patient (two active/reference and one ground electrode). Subjects were fitted with the appropriate correction for a viewing distance of 24 inches and were instructed to fixate on a target at the center of the monitor in front of them.

The stimulus was presented on a gamma corrected Acer V176BM 17-inch monitor, having a refresh rate of 75 frames/second. Luminance output overtime was verified using a luminance meter MavoSpot 2 USB (Gossen, GmbH, Nuremberg; Germany). The pattern stimulus consisted of black/white alternating square bars, reversing at 15 reversals/second (rps) with a duration of 25 seconds for high contrast [HC 85%] and 25 seconds for low contrast [LC 75%] for a total of 50 seconds per eye. The stimulus field subtends a visual angle of 1439.90 arc minutes. Each bar will subtend 22.49 arc minutes, for a total of 64 bars. A red target subtending 50.79 arc minutes was used as a fixation target and was centered on the stimulus field. The luminance of the white bars for 85% and 75% contrast was 204 cd/m^2 and the luminance for black was 20.5 cd/m^2 and 52.5 cd/m^2 yielding a mean luminance of 112.3 cd/m^2 and 128.2 cd/m^2, respectively. All recorded signals underwent band filtration (0.5–100 Hz), amplification (gain = 20,000), and averaging at least 150 frames. The signal was sampled at 1920 samples per second by an analog to digital (A/D) converter. The voltage range of the (A/D) converter was programmed between –5V and +5V. Sweeps contaminated by eye blinks or gross eye saccades were automatically rejected if they exceeded a threshold voltage of 50 μV, and these sections were identified as artifacts in the report. Synchronized single-channel electroretinography was recorded, generating a time series of 384 data points per analysis frame (200 ms). An automatic fast Fourier transformation was applied to the ssPERG waveforms to isolate the desired component at 15 rps. Other frequencies, such as those originating from eye muscles, were rejected. The ssPERG test results were saved in a Structured Query Language (SQL) database and presented in a report form to be used for analysis. For every subject, four pre-programmed full 'contrast sensitivity protocols' were performed sequentially, which consisted of two 25 seconds recordings for each eye: first with high contrast (85%) diffuse retinal

stimulation, then with low contrast (75%) pattern stimulation. The device collected five frames of data per second, totaling 125 frames of data, and the first 10 frames (2 seconds) of data were discarded. For each eye, three ssPERG measurements [Magnitude (Mag), MagnitudeD (MagD), and MagD/Mag ratio] were calculated. Mag (μV) represents the amplitude of the signal strength at the specific reversal rate of 15 Hz in the frequency domain, while MagD (μV) represents an adjusted amplitude of the ssPERG signal impacted by phase variability throughout the waveform recording. A recording where the phase of the response is consistent will produce a MagD value close to that of the Mag, whereas a recording where the phase of the response varies will produce a MagD value lower than that of Mag. This is because averaging responses that are out-of-phase with each other will cause some degree of cancellation. The MagD/Mag ratio is a ratio that is a within-subject representation of the phase consistency of ssPERG. The signal-to-noise ratio (SNR) represents the level of electrical noise compared with the level of the ssPERG signal at 15 Hz.

Statistical Analysis

For all variables of interest, outliers with values ≥3 standard deviations from the mean were excluded from the analyses. Shapiro-Wilk test was used to determine the normality of the distribution for all important variables. ssPERG parameters were subsequently transformed to achieve normality of the distribution. ssPERG parameters achieved normal distribution through the following transformations: a log10 transformation of Mag (Shapiro-Wilk, $p = 0.290$), a log10 transformation for MagD (Shapiro-Wilk, $p = 0.654$), and a cubed transformation for MagD/Mag ratio (Shapiro-Wilk, $p = 0.075$).

Descriptive statistics were used to evaluate continuous and demographic data. Mean and standard deviation values were determined for each ssPERG parameter (Mag, MagD, and MagD/Mag ratio), HFA Swedish Interactive Thresholding Algorithm (SITA) standard (24–2 and 10–2) tests, all RNFLT, GCL/IPL, and macular thickness variables. Associations among continuous variables were analyzed using partial correlations, adjusting for age, sex, intraocular pressure (IOP), central corneal thickness (CCT), and spherical equivalent (SE). Linear regression analyses were used to assess the relationships among ssPERG parameters and OCT derived structural RNFL, GCL/IPL, and macular thickness measures. Statistical Analyses were performed with commercially available software (IBM® SPSS® ver.25.0; SPSS Inc, Chicago, IL, USA).

Results

Cohort Characteristics

This study included 49 eyes of 26 patients with a mean age of 59.86 years. Of these patients, 61.5% were female. Approximately 73.1% of patients identified as white and 15.4% identified as Hispanic. The mean IOP was 17.43 mm Hg and mean deviations (MD) 24–2 and 10–2 MD were 0.00 dB and 0.04 dB, respectively. The mean average retinal nerve fiber layer thickness (avRNFLT) was 90.23 μm. A complete breakdown of cohort characteristics is shown in Table 1.

Table 1: Clinical features and characteristics of the study cohort ($n = 49$ eyes of 26 patients)

Characteristic	*No. (%) or mean ± SD*
Age (years)	59.86 ± 13.1
Sex	
Male	10 (38.5%)
Female	16 (61.5%)
Race	
White	19 (73.1%)
Black	2 (7.7%)
Asian	3 (11.5%)
Other	2 (7.7%)
Ethnicity	
Hispanic	4 (15.4%)
Non-Hispanic	22 (84.6%)
Central corneal thickness (μm)	551.14 ± 32.1
Intraocular pressure (mm Hg)	17.43 ± 4.1
Spherical equivalent (D)	-1.07 ± 2.5
HFA 24-2 visual field index (%)	99.22 ± 0.9
HFA 24-2 MD (dB)	0.00 ± 1.1
HFA 24-2 PSD (dB)	1.56 ± 0.4
HFA 10-2 MD (dB)	0.04 ± 0.9
HFA 10-2 PSD (dB)	1.19 ± 0.2
SD-OCT retinal nerve fiber layer (μm)	90.23 ± 9.8
SD-OCT average GCL/IPL thickness (μm)	79.19 ± 9.6
SD-OCT minimum GCL/IPL thickness (μm)	76.36 ± 6.4

HFA, Humphrey visual field analyzer; SD-OCT, spectral domain optical coherence tomography; MD, mean deviation; PSD, pattern standard deviation; GCL, ganglion cell layer; IPL, inner plexiform layer

Partial Correlation Analyses among ssPERG Parameters and RNFL Thickness Measurements

After controlling for known glaucoma risk factors such as age, sex, CCT, IOP, and SE, a partial correlation analysis between transformed ssPERG parameters and RNFL quadrants and average were performed (Table 2). Both Mag and MagD had positive correlations with the superior and inferior quadrants. The MagD/Mag ratio only had a positive correlation with the superior quadrant ($p = 0.026$) and had no significant correlation with the inferior quadrant ($p = 0.158$). Average RNFL thickness was significantly correlated with Mag ($p = 0.005$) and MagD ($p = 0.007$).

Partial Correlation analyses among ssPERG Parameters and GCL/IPL Thickness Measurements

After controlling for glaucoma risk factors (age, sex, CCT, IOP, and SE), a partial correlation between transformed ssPERG parameters and GCL/IPL thickness measurements were performed (Table 2). Mag had a positive correlation with superior ($p = 0.011$) and superotemporal ($p = 0.019$) and inferonasal ($p = 0.043$) GCL/IPL sectors. MagD and the MagD/Mag ratio had a positive correlation with all GCL/IPL sectors. All three PERG parameters had significant positive correlations with average GCL/IPL thickness and minimum GCL/IPL thickness.

Partial Correlation Analyses among ssPERG Parameters and Macular Thickness Measurements

After controlling for glaucoma risk factors (age, sex, CCT, IOP, and SE), a partial correlation between transformed ssPERG parameters and macular thickness by sectors was performed (Table 2). Mag had a significant positive correlation with all inner macular sectors

Table 2: Partial correlations between transformed ssPERG parameters and OCT variables after controlling for age, sex, central corneal thickness, intraocular pressure, and spherical equivalent

	Magnitude[c]		*MagnitudeD*[c]		*MagD/Mag Ratio*[c]	
OCT variables	*Correlation (r)*	*p*	*Correlation (r)*	*p*	*Correlation (r)*	*p*
RNFL thickness by quadrants						
Superior	0.558	0.001[b]	0.547	0.001[b]	0.394	0.026[a]
Temporal	0.237	0.191	0.161	0.378	0.100	0.587
Inferior	0.413	0.019[a]	0.421	0.017[a]	0.256	0.158
Nasal	-0.010	0.957	0.031	0.868	0.065	0.723
Average RNFL thickness	0.486	0.005[b]	0.464	0.007[b]	0.328	0.067
GCL/IPL thickness by sector						
Superonasal	0.324	0.070	0.414	0.018[a]	0.373	0.036[a]
Superior	0.444	0.011[a]	0.541	0.001[b]	0.520	0.002[b]
Superotemporal	0.413	0.019[a]	0.444	0.011[a]	0.385	0.030[a]
Inferotemporal	0.305	0.089	0.422	0.016[a]	0.467	0.00[b]
Inferior	0.301	0.094	0.446	0.011[a]	0.469	0.007[b]
Inferonasal	0.359	0.043[a]	0.441	0.012[a]	0.381	0.031[a]
Average GCL/IPL thickness	0.369	0.038[a]	0.521	0.002[b]	0.600	<0.001[b]
Minimum GCL/IPL thickness	0.464	0.007[b]	0.598	<0.001[b]	0.605	<0.001[b]
Macular thickness by sector						
Outer superior	0.203	0.250	0.271	0.121	0.277	0.113
Inner superior	0.498	0.003 [b]	0.555	0.001[b]	0.453	0.007[b]
Outer temporal	0.256	0.144	0.270	0.122	0.233	0.184
Inner temporal	0.513	0.002[b]	0.540	0.001[b]	0.379	0.027[a]
Outer inferior	0.028	0.875	0.056	0.753	0.053	0.768
Inner inferior	0.425	0.012[a]	0.451	0.007[b]	0.260	0.138
Outer nasal	0.302	0.082	0.378	0.027[a]	0.363	0.035[a]
Inner nasal	0.437	0.010[b]	0.477	0.004[a]	0.347	0.044[a]

[a] *p*-values <0.05 were considered statistically significant; [b] *p*-values <0.0; [c] Analysis performed using transformed Magnitude, MagnitudeD, and MagD/Mag ratio, respectively; *ssPERG, steady-state pattern electroretinogram;* GCL, ganglion cell layer; IPL, inner plexiform layer; OCT, optical coherence tomography; RGC, retinal ganglion cell; RNFL, retinal nerve fiber layer; Mag, Magnitude

($r > 0.425, p < 0.012$), while MagD had a significant positive correlation with all inner macular sectors ($r > 0.451, p > 0.007$) and the outer nasal sector ($p = 0.027$). The MagD/Mag ratio had a positive correlation with inner superior ($p = 0.007$), outer nasal ($p = 0.035$), inner nasal ($p = 0.044$), and inner temporal ($p = 0.027$) sectors. There was no significant correlation between ssPERG parameters and central subfield thickness (μm), cube volume (mm^2), and cube average thickness (μm).

Hierarchical Stepwise Regression Analysis of ssPERG Parameters and RNFL Thickness Measurements

A hierarchical regression analysis was performed to examine the effect of ssPERG parameters (Mag, MagD, and the MagD/Mag ratio) in predicting RNFL thickness change after controlling glaucoma risk factors (age, sex, CCT, IOP, and SE). Mag significantly predicted superior ($\beta = 20.714$; $p < 0.001$) and inferior ($\beta = 13.024$; $p = 0.013$) RNFL quadrants, as well as avRNFL thickness ($\beta = 9.174$; $p = 0.002$; Table 3). MagD also significantly predicted superior ($\beta = 19.325$; $p < 0.001$) and inferior ($\beta = 11.282$; $p = 0.005$) RNFL quadrants and avRNFL thickness change ($\beta = 8.116$; $p = 0.001$; Table 4). Mag and MagD did not significantly predict temporal and nasal RNFL quadrant thickness change. The MagD/Mag ratio was not predictive of avRNFL thickness or thickness of any specific RNFL quadrants change (Table 5). Regression plots for ssPERG parameters predicting average RNFL thickness can be seen in Supplemental Figure 1.

Hierarchical Stepwise Regression Analysis of ssPERG Parameters and GCL/IPL Thickness Measurements

A hierarchical regression analysis was performed to examine the effect of ssPERG parameters in predicting GCL/IPL thickness after controlling for age, sex, CCT, IOP, and SE. Mag (Table 3), MagD (Table 4), and the MagD/Mag ratio (Table 5) were each significantly predictive of GCL/IPL thickness in all sectors. These ssPERG parameters were also found to be predictive of average and minimum GCL/IPL thicknesses. Regression plots for ssPERG parameters predicting average RNFL thickness can be seen in Supplemental Figure 2.

Hierarchical Regression Analysis of ssPERG Parameters and Macular Thickness

A hierarchical regression analysis was performed to examine the effect of ssPERG parameters in predicting macular thickness after controlling for age, sex, CCT, IOP and SE. Mag was significantly predictive of all inner macular sectors: superior ($\beta = 11.226$; $p = 0.001$), temporal ($\beta = 9.368$; $p = 0.001$), inferior ($\beta = 6.497$; $p = 0.007$), and nasal ($\beta = 10.826$; $p = 0.005$; Table 3). Mag was not predictive of any outer macula sectors. MagD was significantly

Table 3: Associations of Magnitude with OCT variables, controlling for age, sex, intraocular pressure, central corneal thickness, and spherical equivalent

Dependent variable[c]	ΔR^2	*β*	*95% CI*	*p*
RNFL thickness by quadrants				
Superior	0.244	20.714	[10.076–31.352]	<0.001[b]
Temporal	0.016	4.025	[-4.504–12.553]	0.343
Inferior	0.127	13.024	[2.979–23.069]	0.013[a]
Nasal	0.003	1.011	[-5.053–7.075]	0.736
Average RNFL thickness	0.158	9.174	[3.488–14.860]	0.002[b]
GCL/IPL thickness by sector				
Superonasal	0.083	4.968	[0.448–9.487]	0.032[a]
Superior	0.157	6.469	[2.122–10.816]	0.005[b]
Superotemporal	0.147	5.371	[1.545–9.198]	0.007[b]
Inferotemporal	0.073	3.759	[0.355–7.163]	0.032[b]
Inferior	0.052	3.666	[0.278–7.054]	0.035 [a]
Inferonasal	0.076	4.470	[0.623–8.317]	0.024[a]
Average GCL/IPL thickness	0.113	5.097	[0.946–9.249]	0.018[a]
Minimum GCL/IPL thickness	0.189	6.342	[2.325–10.359]	0.003[b]
Macular thickness by sector				
Inner superior	0.212	11.226	[4.755–17.698]	0.001[b]
Inner temporal	0.224	9.368	[4.399–14.337]	0.001[b]
Inner inferior	0.144	6.497	[1.933–11.061]	0.007[b]
Inner nasal	0.189	10.826	[3.571–18.081]	0.005[b]

[a] *p*-values <0.05 were considered statistically significant; [b] *p*-values <0.01; [c] Analysis performed using transformed Magnitude; OCT, optical coherence tomography; GCL, ganglion cell layer; IPL, inner plexiform layer; β, unstandardized beta

predictive of all inner sectors as well as the outer temporal (β = 5.210; $p = 0.013$) and outer nasal sectors (β =7.810; $p = 0.008$; Table 4). The MagD/Mag ratio was predictive of the inner superior (β = 32.609; $p = 0.004$), inner temporal (β = 23.418; $p = 0.016$), and inner nasal (β = 28.510; $p = 0.028$) sectors only.

Discussion

This study demonstrated that the ssPERG parameters Mag, MagD, and the MagD/Mag ratio can serve as potential markers for detecting early glaucomatous changes in glaucoma suspects. It has previously been established that ssPERG parameters Mag and MagD are both repeatable and reproducible, allowing them to be reliably used in clinical practice.[11] Mag and MagD were correlated with the superior and inferior RNFL quadrants while the MagD/Mag ratio was only correlated with the superior RNFL quadrant. In the linear regression analysis, Mag and MagD were significantly predictive of superior and inferior RNFL quadrant and avRNFL thicknesses. The Mag/MagD ratio was not predictive of any RNFL thicknesses, however, it has been reported to be the least reliable ssPERG measurement.[11] Similarly, all ssPERG parameters were correlated with GCL/IPL and macular thinning. Mag, MagD, and the MagD/Mag ratio were predictive of all the GCL/IPL sector thicknesses and most of the inner macula sector thicknesses in the linear regression analysis. Only MagD was significantly predictive of the outer macular thickness sector.

It has been reported that amplitude, measured in this study with Mag, and latency, measured in this study as MagD, are essentially uncoupled in ssPERG and each represents separate aspects of RGC activity.[21] The authors hypothesized that phase delays in the absence of amplitude were secondary to synaptic dysfunction.[21] The ability of MagD, but not Mag, to predict RGC dysfunction suggests that in glaucoma suspects, there may be early signs of RGC synaptic dysfunction in the outer macula prior to any RGC loss that can be detected on SD-OCT. Additionally, MagD had significant correlations with a greater number of GCL/IPL sector thicknesses than Mag, further indicating that ssPERG could be detecting RGC signaling dysfunction in these sectors prior to RGC death.

Patients with optic disk abnormalities or known glaucoma risk factors with normal perimetry and SD-OCT findings may be regarded as "glaucoma suspects" due to their increased risk for glaucomatous optic nerve changes in the future. All the patients in this study had SD-OCT values for RNFL, GCL/IPL, and macular thickness that fell within the normative data ranges specified by the Zeiss Cirrus OCT manual.[22] Previous studies of glaucoma suspects have reported mean avRNFL thicknesses ranging from 74.8–101 µm, which is in agreement with the mean avRNFL thickness in this study.[23-25] Patients in this study also experienced no visual field deficits but had clinical features or risk factors that would classify them as glaucoma suspects.

Previous studies have identified a reduction in ssPERG amplitude prior to visual field changes in glaucoma suspects.[14,26] Bode et al. found that the ssPERG ratio had a sensitivity and specificity of 75% and 76%, respectively and that ssPERG could detect glaucoma in patients 4 years before the onset of any visual field changes.[27,28] In addition, studies have suggested the RGC dysfunction detected by ssPERG may be potentially reversible, making ssPERG a useful clinical tool in detecting at-risk patients.[6,14] Because ssPERG has been shown to provide reliable and repeatable measurements, researchers have started to use it to assess RGC dysfunction in patients with a variety of optic neuropathies.[11,18] Tirsi et al. found that Mag and MagD had significant associations with optic nerve head morphology and could

Table 4: Associations of MagnitudeD with OCT variables, controlling for age, sex, intraocular pressure, central corneal thickness, and spherical equivalent

Dependent variable[c]	ΔR^2	*β*	*95% CI*	*p*
RNFL thickness by quadrants				
Superior	0.259	19.325	[11.193–27.458]	<0.001[b]
Temporal	0.004	1.528	[-5.041–8.096]	0.639
Inferior	0.127	11.282	[3.652–18.913]	0.005[b]
Nasal	0.006	1.212	[-3.388–5.812]	0.596
Average RNFL thickness	0.156	8.116	[3.773–12.459]	0.001[b]
GCL/IPL thickness by sector				
Superonasal	0.107	4.779	[1.435–8.123]	0.006[b]
Superior	0.190	6.200	[3.042–9.357]	<0.001[b]
Superotemporal	0.149	4.671	[1.785–7.557]	0.002[b]
Inferotemporal	0.097	3.759	[1.264–6.255]	0.004[b]
Inferior	0.083	3.944	[1.495–6.393]	0.002[b]
Inferonasal	0.093	4.267	[1.382–7.152]	0.005[b]
Average GCL/IPL thickness	0.174	5.407	[2.438–8.376]	0.001[b]
Minimum GCL/IPL thickness	0.251	6.359	[3.508–9.210]	<0.001[b]
Macular thickness by sector				
Inner superior	0.210	9.261	[4.424–14.098]	<0.001[b]
Inner temporal	0.196	7.077	[3.224–10.929]	0.001[b]
Inner inferior	0.132	5.283	[1.781–8.785]	0.004[b]
Inner nasal	0.201	8.984	[3.535–14.434]	0.002[b]

[a] *p*-values <0.05 were considered statistically significant; [b] *p*-values <0.01; [c] Analysis performed using transformed MagnitudeD; OCT, optical coherence tomography; GCL, ganglion cell layer; IPL, inner plexiform layer; β, unstandardized beta

Table 5: Associations of MagD/Mag ratio with OCT variables, controlling for age, sex, intraocular pressure, central corneal thickness, and spherical equivalent

Dependent variable[c]	ΔR^2	*β*	*95% CI*	*p*
RNFL thickness by quadrants				
Superior	0.054	38.260	[-6.449–82.968]	0.091
Temporal	0.001	2.668	[-26.863–32.200]	0.855
Inferior	0.034	25.548	[-12.007–63.103]	0.175
Nasal	0.005	4.822	[-15.810–25.454]	0.637
Average RNFL thickness	0.032	15.851	[-6.692–38.393]	0.162
GCL/IPL thickness by sector				
Superonasal	0.079	18.157	[2.919–33.395]	0.021[a]
Superior	0.140	23.473	[8.763–38.182]	0.003[b]
Superotemporal	0.073	14.703	[0.426–28.981]	0.044[a]
Inferotemporal	0.090	16.600	[4.976–28.223]	0.007[b]
Inferior	0.072	16.400	[5.875–26.925]	0.003[b]
Inferonasal	0.060	15.321	[1.972–28.669]	0.026[a]
Average GCL/IPL thickness	0.190	25.127	[12.278–37.976]	<0.001[b]
Minimum GCL/IPL thickness	0.211	25.965	[12.689–39.241]	<0.001[b]
Macular thickness by sector				
Inner superior	0.146	32.609	[11.111–54.106]	0.004[b]
Inner temporal	0.106	23.418	[4.646–42.190]	0.016[a]
Inner inferior	0.050	14.635	[-2.512–31.781]	0.092
Inner nasal	0.109	28.510	[3.227–53.792]	0.028[a]

[a] *p*-values <0.05 were considered statistically significant; [b] *p*-values <0.01; [c] Analysis performed using transformed MagD/Mag ratio; Mag, Magnitude; MagD, Magnitude D; OCT, optical coherence tomography; GCL, ganglion cell layer; IPL, inner plexiform layer; β, unstandardized beta

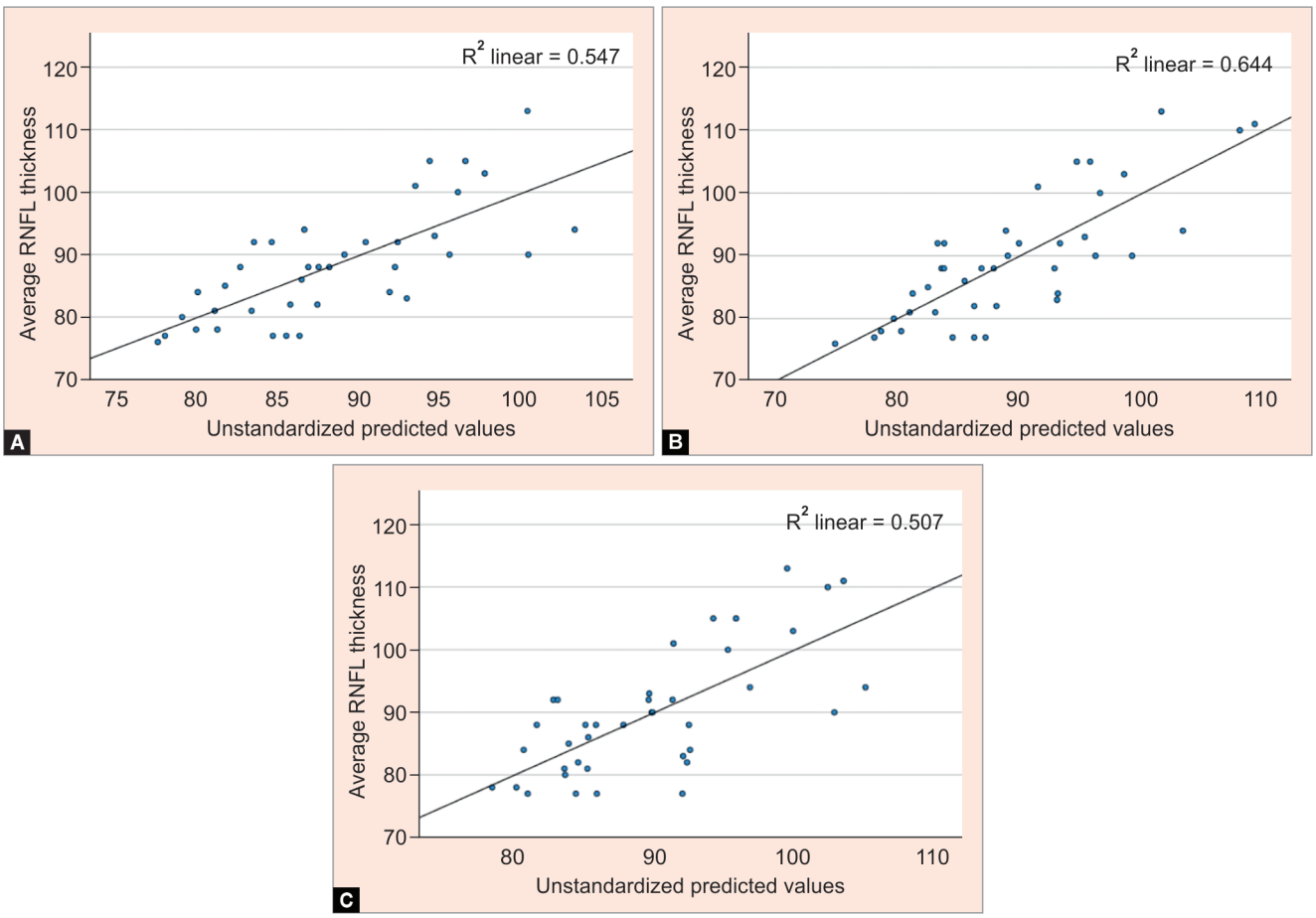

Figs 1A to C: Relationships between pattern electroretinogram parameters and average retinal nerve fiber layer (avRNFL) thickness after adjusting for age, sex, intraocular pressure, central corneal thickness, and spherical equivalent. (A) Magnitude (R^2 = 0.547); (B) MagnitudeD (R^2 = 0.644); (C) MagnitudeD/Magnitude ratio (R2 = 0.507)

predict changes in rim area and Bruch's membrane opening-minimum rim width in preperimetric glaucoma patients.[7] Kudrna et al. used the ssPERG measurements MagD and the MagD/Mag ratio to monitor RGC function in patients with a pressure-lowering periocular device.[29] These studies along with this present study suggest that ssPERG may serve as a valuable tool for monitoring the progression of the disease, especially in glaucoma suspects, to detect early changes.

The findings in this current study are consistent with the recent literature, which has demonstrated that common changes in glaucoma include superior and inferior RNFL thinning and GCL/IPL thinning.[2,30-33] It has been demonstrated that when RGCs are dysfunctional or damaged in glaucoma, the axonal loss can precede RGC soma loss.[34] This decrease in axon number can be measured reliably using OCT, seen as a thinning of the RNFL.[35] It has also been proposed that there are significant dendritic changes of the RGCs that occur in glaucoma such as retraction of the branches, reduced complexity, and loss of synapses.[36,37] These changes that result in the pruning of dendrites would manifest as thinning of the IPL, seen on OCT. RGC soma loss, as a result of apoptosis, results in thinning of the GCL.[37] To summarize these changes, glaucomatous damage leads to decreased RNFL and GCL/IPL thicknesses on OCT. Although OCT is a reliable test in detecting glaucomatous damage, glaucoma suspects can still have normal OCTs.[9] The findings in this study suggest that reductions in the ssPERG parameters correlate with early glaucomatous changes such as RNFL and GCL/IPL thinning and support that the patient population in this study are showing suggestive early glaucomatous changes despite normal OCT and perimetry.

The correlation between reduced ssPERG parameters and reduced total macular thickness found in this study is also in line with previous studies that have found reduced macular thickness in patients with glaucoma.[38,39] It has been suggested that this is secondary to the thinning in the GCL/IPL layers.[39] The macular region has been reported to contain approximately 50% of all RGCs, which are reduced in glaucoma, and there is a strong association between macular RGC density and GCL/IPL thickness.[40,41] Interestingly, ssPERG had significant correlations with all the inner sector thicknesses and had a much weaker correlation with the outer sector thicknesses of the macula in this study. It is plausible that there may be a higher concentration of RGCs in the inner three-millimeter region of the macula measured by the Zeiss Cirrus OCT machines. A previous study by Hood et al. found that the GCL/IPL layer was thickest at the five degrees radius point from the macula, which appears to align with the inner region measured by the Zeiss Cirrus OCT.[42] Therefore, the inner sectors would experience greater decreases in thickness with greater loss of RGCs compared to outer sectors, leading to more significant correlations seen on ssPERG.

Like all retrospective studies, there are limitations to this current study due to potential biases in patient selection. The sample size of this study was also relatively small. Therefore, larger, prospective investigations should be performed to further confirm the findings in this study. There is also a lack of a standardized international

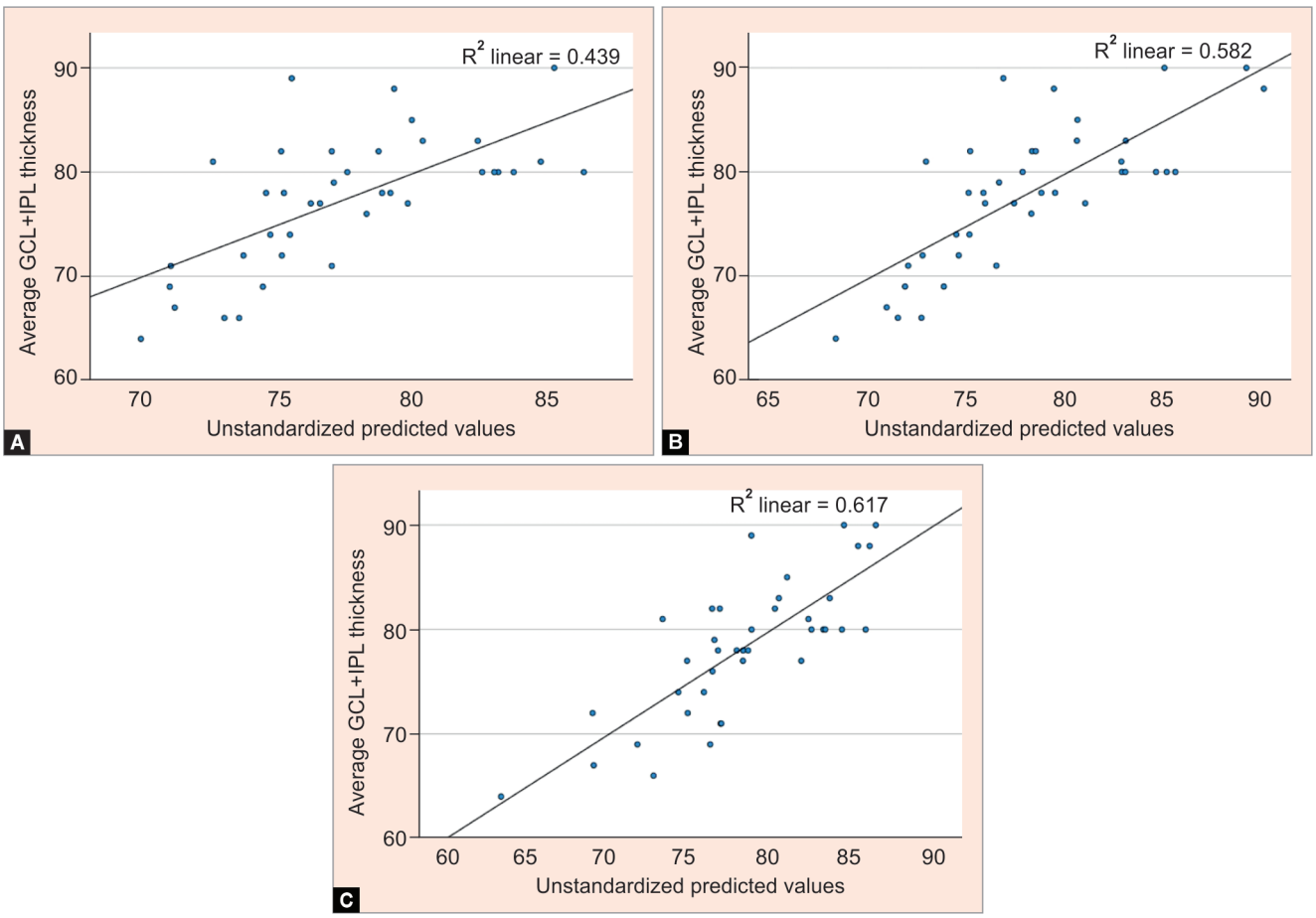

Figs 2A to C: Relationships between pattern electroretinogram parameters and average ganglion cell layer inner plexiform layer (avGCL-IPL) thickness after adjusting for age, sex, intraocular pressure, central corneal thickness, and spherical equivalent. (A) Magnitude (R^2 = 0.439); (B) MagnitudeD (R^2 = 0.582); (C) MagnitudeD/Magnitude ratio (R^2 = 0.617)

reference range for ssPERG measurements and there are several subjective factors that influence the Mag, MagD, and MagD/Mag ratio including the patient's ability to concentrate and adequate eye fixation.[3] Despite these limitations, the findings of this study suggest that Mag, MagD, and the MagD/Mag ratio are sensitive markers of early glaucomatous changes and can be predictive of RNFL, GCL/IPL, and macular thinning in glaucoma suspects.

Conclusion

Abnormalities in ssPERG parameters, an indication of RGC dysfunction, are associated with structural damage visualized on SD-OCT. However, even when SD-OCT thickness measurements fall within normal ranges, glaucoma suspects can still display functional changes. Functional changes preceded structural damage. These abnormalities on ssPERG in GS suggest a potential increased risk of future glaucoma development. Therefore, it is important to monitor these patients prior to any detectable SD-OCT or VF changes to provide early interventions when the functional damage is possibly reversible.

Clinical Significance

In this study of glaucoma suspects, ssPERG had significant correlations with RNFL, GCL/IPL, and macular thicknesses. ssPERG was also predictive of these changes as well in linear regression analysis. Therefore, ssPERG may serve as a valuable tool for early detection of disease and monitoring disease progression in glaucoma suspects.

Author Contribution

#These authors contributed equally to this work.

Orcid

Andrew Tirsi https://orcid.org/0000-0002-8424-7574
Daniel Zhu https://orcid.org/0000-0001-6569-9623

References

1. Fry LE, Fahy E, Chrysostomou V, et al. The coma in glaucoma: Retinal ganglion cell dysfunction and recovery. Prog Retin Eye Res 2018;65:77–92. DOI: 10.1016/j.preteyeres.2018.04.001
2. Zivkovic M, Dayanir V, Zlatanovic M, et al. Ganglion cell-inner plexiform layer thickness in different glaucoma stages measured by optical coherence tomography. Ophthalmic Res 2018;59(3):148–154. DOI: 10.1159/000478052
3. Park K, Kim J, Lee J. Measurement of macular structure-function relationships using spectral domain-optical coherence tomography (SD-OCT) and pattern electroretinograms (PERG). PLoS One 2017;12(5):e0178004. DOI: 10.1371/journal.pone.0178004
4. Ventura LM, Sorokac N, De Los Santos R, et al. The relationship between retinal ganglion cell function and retinal nerve fiber thickness in early glaucoma. Invest Ophthalmol Vis Sci 2006;47(9):3904–3911. DOI: 10.1167/iovs.06-0161
5. Tielsch JM, Katz J, Singh K, et al. A Population-based evaluation of glaucoma screening: the Baltimore eye survey. Am J Epidemiol 1991;134(10):1102–1110. DOI: 10.1093/oxfordjournals.aje.a116013

6. Salgarello T, Giudiceandrea A, Calandriello L, et al. Pattern electroretinogram detects localized glaucoma defects. Transl Vis Sci Technol 2018;7(5):6. DOI: 10.1167/tvst.7.5.6
7. Tiris A, Gliagias V, Moehringer J, et al. Pattern electroretinogram parameters are associated with optic nerve morphology in preperimeteric glaucoma after adjusting for disc area. J Ophthalmol 2021;2021: 8025337. DOI: 10.1155/2021/8025337
8. Vajaranant TS, Anderson RJ, Zelkha R, et al. The relationship between macular cell layer thickness and visual function in different stages of glaucoma. Eye (Lond) 2011;25(5):612–618. DOI: 10.1038/eye.2011.17
9. Chang RT, Singh K. Glaucoma suspect: diagnosis and management. Asia-Pac J Ophthalmol 2016;5(1):32–37. DOI: 10.1097/APO.0000000000000173
10. Kerrigan-Baumrind LA, Quigley HA, Pease ME, et al. Number of ganglion cells in glaucoma eyes compared with threshold visual field tests in the same persons. Invest Ophthalmol Vis Sci 2000;41(3):741–748.
11. Gillmann K, Mansouri K, Rao HL, et al. A prospective evaluation of the repeatability and reliability of new steady-state pattern electroretinogram parameters. J Glaucoma 2018;27(12):1079–1085. DOI: 10.1097/IJG.0000000000001103
12. Porciatti V, Ventura LM. Normative data for a user-friendly paradigm for pattern electroretinogram recording. Ophthalmology 2004;111(1):161–168. DOI: 10.1016/j.ophtha.2003.04.007
13. Fredette M-J, Anderson DR, Porciatti V, et al. Reproducibility of pattern electroretinogram in glaucoma patients with a range of severity of disease with the new glaucoma paradigm. Ophthalmology 2008;115(6):957–963. DOI: 10.1016/j.ophtha.2007.08.023
14. Ventura LM, Porciatti V, Ishida K, et al. Pattern electroretinogram abnormality and glaucoma. Ophthalmology 2005;112(1):10–19. DOI: 10.1016/j.ophtha.2004.07.018
15. O'Donaghue E, Arden GB, O'Sullivan F, et al. The pattern electroretinogram in glaucoma and ocular hypertension. Br J Ophthalmol 1992;76(7):387–394. DOI: 10.1136/bjo.76.7.387
16. Ambrosio G, Arienzo G, Aurilia P, et al. Pattern electroretinograms in ocular hypertension. Doc Ophthalmol 1988;69(2):161–165. DOI: 10.1007/BF00153697
17. Luttrull JK. Improved retinal and visual function following pan macular subthreshold diode micropulse laser for retinitis pigmentosa. Eye (Lond) 2018;32(6):1099–1110. DOI: 10.1038/s41433-018-0017-3
18. Resende AF, Sanvicente CT, Eshraghi H, et al. Test-retest repeatability of the pattern electroretinogram and flicker electroretinogram. Doc Ophthalmol 2019;139(3):185–195. DOI: 10.1007/s10633-019-09707-5
19. Mwanza J-C, Oakley JD, Budenz DL, et al. Macular ganglion cell-inner plexiform layer: automated detection and thickness reproducibility with spectral domain-optical coherence tomography in glaucoma. Invest Ophthalmol Vis Sci 2011;52(11):8323–8329. DOI: 10.1167/iovs.11-7962
20. Shengelia A, Tello C, Siegfried J, et al. Diopsys NOVA-ERG system: Reference values of healthy subjects and thresholds for discriminating abnormal visual function from healthy subjects. ARVO 2015 Annual Meeting, Abstract/Poster #1030-B0164.
21. Porciatti V, Ventura LM. Physiological significance of steady-state pattern electroretinogram losses in glaucoma: clues from simulation of abnormalities in normal subjects. J Glaucoma 2009;18(7):535–542. DOI: 10.1097/IJG.0b013e318193c2e1
22. Carl Zeiss Meditec, Inc. CIRRUS HD-OCT User Manual. Published 2015. Accessed August 19, 2021. https://www.zeiss.co.uk/content/dam/Meditec/gb/Chris/Refractive-Business-Builder/2018Updates/UserGuides/oct_usermanual.pdf
23. Lalezary M, Medeiros FA, Weinreb RN, et al. Baseline optical coherence tomography predicts the development of glaucomatous change in glaucoma suspects. Am J Ophthalmol 2006;142(4):576–582. DOI: 10.1016/j.ajo.2006.05.004
24. Stagg BC, Medeiros FA. A comparison of OCT parameters in identifying glaucoma damage in eyes suspected of having glaucoma. Ophthalmol Glaucoma 2020;3(2):90–96. DOI: 10.1016/j.ogla.2019.11.008
25. Miki A, Medeiros FA, Weinreb RN, et al. Rates of retinal nerve fiber layer thinning in glaucoma suspect eyes. Ophthalmology 2014;121(7):1350–1358. DOI: 10.1016/j.ophtha.2014.01.017
26. Bayer AU, Maag K-P, Erb C. Detection of optic neuropathy in glaucomatous eyes with normal standard visual fields using a test battery of short-wavelength automated perimetry and pattern electroretinography. Ophthalmology 2002;109(7):1350–1361. DOI: 10.1016/s0161-6420(02)01100-4
27. Bode SFN, Thomas Jehle, Bach M. Pattern electroretinogram in glaucoma suspects: new findings from a longitudinal study. Invest Ophthalmol Vis Sci 2011;52(7):4300–4306. DOI: 10.1167/iovs.10-6381
28. Banitt MR, Ventura LM, Feuer WJ, et al. Progressive loss of retinal ganglion cell function precedes structural loss by several years in glaucoma suspects. Invest Ophthalmol Vis Sci 2013;54(3):2346–2352. DOI: 10.1167/iovs.12-11026
29. Kudrna JJ, Ferguson TJ, Swan RJ, et al. Short-term steady-state pattern electroretinography changes using a multi-pressure dial in ocular hypertensive, glaucoma suspect, and mild open-angle glaucoma patients: a randomized, controlled, prospective, pilot study. Ophthalmol Ther 2020;9(4):981–992. DOI: 10.1007/s40123-020-00302-5
30. Abrol S, Gupta S, Naik M, et al. Can we corroborate peripapillary rnfl analysis with macular gcipl analysis? our 2-year experience at a single-centre tertiary healthcare hospital using two oct machines and a review of literature. Clin Ophthalmol 2020;14:3763–3774. DOI: 10.2147/OPTH.S266112
31. Leung CKS, Yu M, Weinreb RN, et al. Retinal nerve fiber layer imaging with spectral-domain optical coherence tomography: a prospective analysis of age-related loss. Ophthalmology 2012;119(4):731–737. DOI: 10.1016/j.ophtha.2011.10.010
32. Choi JA, Park H-YL, Jung K-I, et al. Difference in the Properties of Retinal Nerve Fiber Layer Defect Between Superior and Inferior Visual Field Loss in Glaucoma. Invest Ophthalmol Vis Sci 2013;54(10):6982–6990. DOI: 10.1167/iovs.13-12344
33. Kim HJ, Lee S-Y, Park KH, et al. Glaucoma diagnostic ability of layer-by-layer segmented ganglion cell complex by spectral-domain optical coherence tomography. Invest Ophthalmol Vis Sci 2016;57(11):4799–4805. DOI: 10.1167/iovs.16-19214
34. Soto I, Pease ME, Son JL, et al. Retinal ganglion cell loss in a rat ocular hypertension model is sectorial and involves early optic nerve axon loss. Invest Ophthalmol Vis Sci 2011;52(1):434–441. DOI: 10.1167/iovs.10-5856
35. Mead B, Tomarev S. Evaluating retinal ganglion cell loss and dysfunction. Exp Eye Res 2016;151:96–106. DOI:10.1016/j.exer.2016.08.006
36. Agostinone J, Di Polo A. Retinal ganglion cell dendrite pathology and synapse loss: implications for glaucoma. Prog Brain Res 2015;220:199–216. DOI: 10.1016/bs.pbr.2015.04.012
37. Weber AJ, Kaufman PL, Hubbard WC. Morphology of Single Ganglion Cells in the Glaucomatous Primate Retina. Invest Ophthalmol Vis Sci 1998;39(12): 2304–2320.
38. Greenfield DS. Macular thickness changes in glaucomatous optic neuropathy detected using optical coherence tomography. Arch Ophthalmol 2003;121(1):41–46. DOI: 10.1001/archopht.121.1.41
39. Zeimer R, Asrani S, Zou S, et al. Quantitative detection of glaucomatous damage at the posterior pole by retinal thickness mapping. A pilot study. Ophthalmology. 1998;105(2):224–231. DOI: 10.1016/S0161-6420(98)92743-9
40. Antwi-Boasiako K, Carter-Dawson L, Harwerth R, et al. The relationship between macula retinal ganglion cell density and visual function in the nonhuman primate. Invest Ophthalmol Vis Sci 2021;62(1):5. DOI: 10.1167/iovs.62.1.5
41. Zhang C, Tatham AJ, Weinreb RN, et al. Relationship between ganglion cell layer thickness and estimated retinal ganglion cell counts in the glaucomatous macula. Ophthalmology 2014;121(12):2371–2379. DOI: 10.1016/j.ophtha.2014.06.047
42. Hood DC, Raza AS, de Moraes CGV, et al. Glaucomatous damage of the macula. Prog Retin Eye Res 2013;32:1–21. DOI: 10.1016/j.preteyeres.2012.08.003